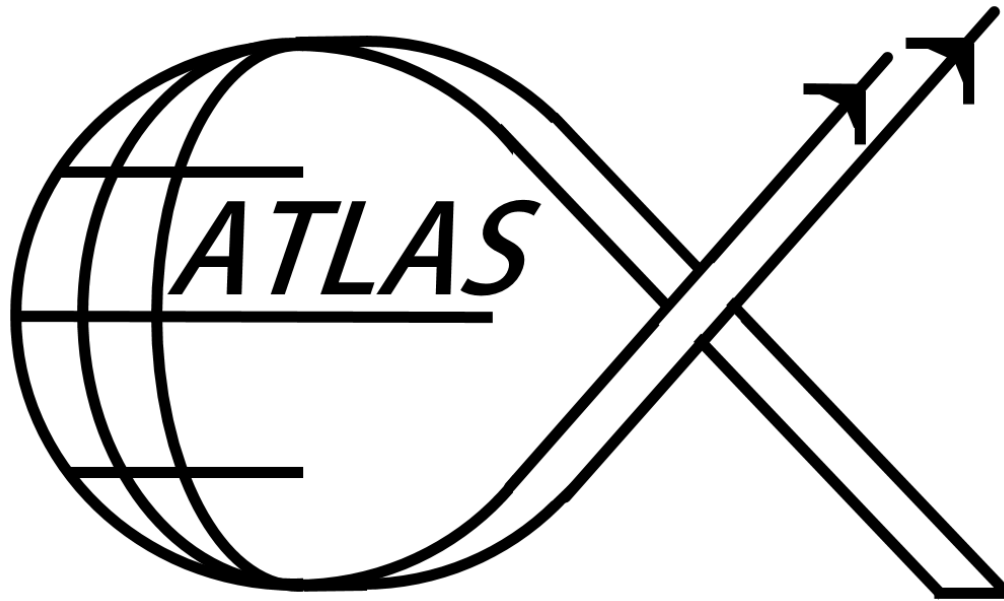


AG-16 Dragonfly Wind Tunnel Test Report

30 November 2016



Prepared by:

John Rangel

ATLAS team members:

Grayson Ridge

Suh Sukongnwi

Tyler Sandman

Gabriel Aguilar

Diane Ngyuen

Romi Patel

Contents

List of Figures	3
List of Tables	3
Nomenclature:	4
Overview:	5
Test Objectives:	5
Data processing and background:	6
Aircraft Geometry:	7
Aircraft Construction:	8
Wind Tunnel Tests:	12
Test Matrix and Test Procedures:	13
Aerodynamic and longitudinal behavior testing	13
Directional stability testing	13
Control surface effectiveness	14
Engine and propeller effects on control surface effectiveness	14
Theoretical results:	15
Results and discussion:	17
Lift and drag analysis:	17
Aircraft stability	18
Control surface effectiveness	19
Propwash effects	21
Appendix A: Wind tunnel analysis description and Github repository	23

List of Figures

- Figure 1: Dragonfly fuselage and jig frame CAD model (page 9)*
- Figure 2: Dragonfly fuselage under construction (page 9)*
- Figure 3: Dragonfly fuselage under construction (page 10)*
- Figure 4: Wind tunnel sting inside the aircraft fuselage CAD view (page 10)*
- Figure 5: Wind tunnel sting inside the aircraft fuselage (page 11)*
- Figure 6: Full aircraft setup in LSWT (page 13)*
- Figure 7: LSWT layout (page 14)*
- Figure 8: XFLR alpha sweep results – CL vs CD and CL vs Alpha sweep (page 15)*
- Figure 9: XFLR alpha sweep results – CM vs Alpha (page 15)*
- Figure 10: XFLR rolling, yawing moment coefficients versus beta angle sweep (page 16)*
- Figures 11 and 12: Dragonfly lift and drag characteristics (page 17)*
- Figure 13: e calculation using area minimization (page 18)*
- Figure 14: Dragonfly stability curves (page 19)*
- Figure 15: Control surface effectiveness (page 20)*
- Figure 16: prop wash effects on elevator (page 20)*
- Figure 17: prop wash effects on rudders (page 20)*

List of Tables

- Table 1: Wind Tunnel primary objectives (page 5)*
- Table 2: Stability requirements (page 7)*
- Table 3: Dragonfly overall characteristics: (page 7)*
- Table 4: Airplane Geometry: (page 8)*
- Table 5: Task Mark XIII measurement ranges and uncertainties (body frame) (page 12)*
- Table 6: Wind Tunnel test symbols and values (page 13)*
- Table 7: Lift and drag values (page 17)*
- Table 8: stability values (page 19)*
- Table 9: control surface deflection conventions (page 19)*
- Table 10: control surface effectiveness (page 20)*
- Table 11: moment difference at zero and max throttle (page 21)*

Nomenclature:

Symbol	Meaning
$C_{L\alpha}$	Change in aircraft lift coefficient with angle of attack
$C_{D\alpha}$	Change in aircraft drag coefficient with angle of attack
α_{stall}	Aircraft stall angle of attack
$C_{M\alpha}$	Change in aircraft moment coefficient with angle of attack
$C_{n\beta}$	Change in yaw moment coefficient with yaw angle
$C_{l\beta}$	Change in roll moment coefficient with yaw angle
$C_{l\delta_{Aileron}}$	Change in rolling moment coefficient with aileron deflection
$C_{m\delta_{Elevator}}$	Change in pitching moment coefficient with elevator deflection
$C_{n\delta_{Rudder}}$	Change in yawing moment coefficient with rudder deflection
L	Lift (wind frame)
D	Drag (wind frame)
N	Normal force (body frame)
A	Axial force (body frame)
α	Vehicle angle of attack
SM	Static margin
\bar{x}_{AC}	X location of aerodynamic center, normalized by reference chord
\bar{x}_b	Distance from aircraft nose to internal balance, normalized by reference chord
C_{M_B}	Coefficient of moment about the internal balance
C_L	Lift coefficient

Overview:

Wind tunnel tests were conducted on a 1:6 scale RC version of the ATLAS AG-16 Dragonfly at various flight conditions and model configurations. The collected data verified the model's calculated performance and stability. Engine-on tests confirmed negligible prop-wash effects on the horizontal and vertical tails. Profile and pressure drag led to lower efficiency and a smaller max lift-over-drag ratio than originally expected, but the effect on RC flight performance is expected to be negligible. ATLAS' wind tunnel test took place November 15, 2016 at the Oran W. Nicks Low Speed Wind Tunnel in College Station, Texas. "Dragonfly" or "Scaled Dragonfly" refers to the 1:6 scale model.

Test Objectives:

Wind tunnel test data was used to verify four aspects of the scaled Dragonfly's design:

1. Aerodynamic behavior
2. Longitudinal stability
3. Directional stability
4. Control surface effectiveness

Each aspect consists of several primary objectives. The objectives for each aspect are listed in Table 1.

Table 1: Wind Tunnel primary objectives

Design aspect	Primary objectives
Aerodynamic behavior	<ul style="list-style-type: none">• Determine aircraft $C_{L\alpha}$• Generate drag polar• Determine Oswald's efficiency factor e• Determine α_{stall}• Verify aircraft wing symmetry• Verify aircraft control surface symmetry
Longitudinal stability	<ul style="list-style-type: none">• Determine aircraft aerodynamic center• Determine aircraft center of gravity• Determine static margin• Determine $C_{M\alpha}$
Directional stability	<ul style="list-style-type: none">• Determine $C_{n\beta}$, or weathercock stability coefficient• Determine $C_{l\beta}$, or lateral stability coefficient
Control surface effectiveness	<ul style="list-style-type: none">• Determine $C_{l\delta_{Aileron}}$• Determine $C_{m\delta_{Elevator}}$• Determine $C_{n\delta_{Rudder}}$• Determine propwash effects on control surface effectiveness

Data processing and background:

The wind tunnel provides force and moment measurements in the aircraft body frame, as well as environment measurements such as temperature, pressure and vehicle orientation. Wind tunnel moments are measured about the balance moment center. The normal and axial force measurements can be translated into lift and drag body frame measurements with the following equations:

$$L = -N\cos(\alpha) + A\sin(\alpha)$$

$$D = N\sin(\alpha) + A\cos(\alpha)$$

The wind tunnel provides ‘pseudo-coefficients’ – force divided by dynamic pressure – in the wind frame and in the body frame. The pseudo-coefficients can be converted into dimensionless coefficients by dividing them by reference areas or reference lengths. Equation 3 demonstrates how a force pseudo-coefficient is normalized by dividing it by the aircraft’s reference area. Equation 4 demonstrates how a moment coefficient is normalized by dividing it by the product of the aircraft’s reference area and reference chord. Note that an accent mark ‘ ’ denotes a pseudo-coefficient.

$$C_{force} = \frac{c'_x}{S_{ref}} \quad C_{moment} = \frac{c'_{moment}}{S_{ref}c_{ref}}$$

The measured moments must be transferred from the balance moment center to the aircraft center of gravity using the following equations:

$$C_{m_{cg}} = C_{m_{BMC}} - C_L \frac{x_b - x_{cg}}{c_{ref}} \quad C_{n_{cg}} = C_{n_{BMC}} + C_Y \frac{x_b - x_{cg}}{b}$$

It is assumed that $C_{l_{cg}} = C_{l_{BMC}}$ because z_{cg} is sufficiently close to x_{bz} ; thus no moment transfer is needed.

Aircraft aerodynamic performance is primarily judged by how the lift, drag and moment coefficients change with respect to alpha:

$$C_{L\alpha} = \frac{\Delta C_L}{\Delta \alpha} \quad C_{D\alpha} = \frac{\Delta C_D}{\Delta \alpha} \quad C_{M\alpha} = \frac{\Delta C_M}{\Delta \alpha}$$

Control surface effectiveness is similarly judged. The ailerons, elevator and rudder are used to change the rolling, pitching and yawing moments, respectively. Their ability to do so is evaluated through control coefficient derivatives – the way a moment changes with respect to a control surface deflection:

$$C_{l_{\delta_{Aileron}}} = \frac{\Delta C_l}{\Delta \delta_{Aileron}} \quad C_{m_{\delta_{Elevator}}} = \frac{\Delta C_m}{\Delta \delta_{Elevator}} \quad C_{n_{\delta_{Rudder}}} = \frac{\Delta C_n}{\Delta \delta_{Rudder}}$$

The static margin offers a straightforward way to judge longitudinal static stability. The static margin is calculated by dividing the difference between the aircraft’s AC and CG by the reference chord:

$$SM = \frac{x_{AC} - x_{CG}}{\bar{c}}$$

Directional stability is judged by how the yawing moment changes with respect to beta, or sideslip:

$$C_{n_\beta} = \frac{\Delta C_n}{\Delta \beta} \quad C_{l_\beta} = \frac{\Delta C_l}{\Delta \beta}$$

A positive C_{n_β} and a negative C_{l_β} correspond to directional stability. The coefficient rate derivative signs necessary for stability are summarized in Table 2.

Table 2: Stability requirements

Parameter	Requirement
C_{M_α}	-
SM	15% - 18%
C_{n_β}	+
C_{l_β}	-

The x-location of the aerodynamic center can be calculated from collected wind tunnel data through the following equation:

$$\bar{x}_{AC} = \bar{x}_b - \frac{\frac{\partial}{\partial \alpha} C_{M_B}}{\frac{\partial}{\partial \alpha} C_L}$$

Where \bar{x}_{AC} is the x-location of the aerodynamic center divided by the wing chord, \bar{x}_b is the distance from the aircraft nose to the internal balance and C_{M_B} is the measured moment about the internal balance. A detailed derivation of the aerodynamic center location can be found in Yogesh Babbar's "Derivation of Aerodynamic Center Location from Wind Tunnel Data," attached in Appendix A.

Aircraft Geometry:

The overall aircraft characteristics and materials are given in Table 2. Detailed characteristics are given in Table 3.

Table 3: Dragonfly overall characteristics:

Parameter	Value	Units
Wing span	5.5	ft
Nose to tail length	4.5	ft
Dry weight*	10	lb

*Estimate based on the CAD model current at time of press.

Table 4: Aircraft Geometry:

Aircraft component	Geometry	Value	Units
Wing	Span (tip to tip)	5.5	ft
*high density foam	Chord	0.75	ft
	Airfoil	4415	--
	Area	4.125	ft2
	Aspect Ratio	7.3	--
	Sweep	0.0	deg
	Incidence	0.0	deg
	Taper Ratio	1.0	--
Horizontal Tail	Span	1.42	ft
*high density foam	Chord	0.5	ft
	Airfoil	0009	--
	Area	0.71	ft2
	Aspect Ratio		--
	Sweep	0.0	deg
	Incidence	0.0	deg
	Taper Ratio	1.0	--
Vertical Tail (2)	Span	0.5	ft
*high density foam	Root chord	0.5	ft
	Airfoil	0009	--
	Area	0.2	ft2
	Taper ratio	0.6	--
	Sweep	26.5	deg
Fuselage	Length	2.27	ft
*plywood, bass wood and balsa wood	Width	0.65	ft
	Height	0.75	ft
Boom	Length	1.59	ft
* carbon fiber rods	Diameter	0.0625	ft

Aircraft Construction:

The scaled Dragonfly does not differ substantially from the original design outside of the 1:6 scale. Air intake and exhaust ports were designed to cool the batteries and engine, and the empennage boom was slightly extended to give greater elevator and rudder control authority. The fuselage frame was made of plywood bulkheads and bent basswood longerons. Balsa wood sheets form the fuselage surface. The entire fuselage is covered in monokote for aesthetics. The wing, horizontal tail and vertical tails are made of high density foam vacuum-packed in carbon fiber cloth. The two empennage booms are made from woven carbon fiber rods.

Figure 1 shows ATLAS' fuselage CAD model with jig frame. Figure 2 shows a partially constructed fuselage.

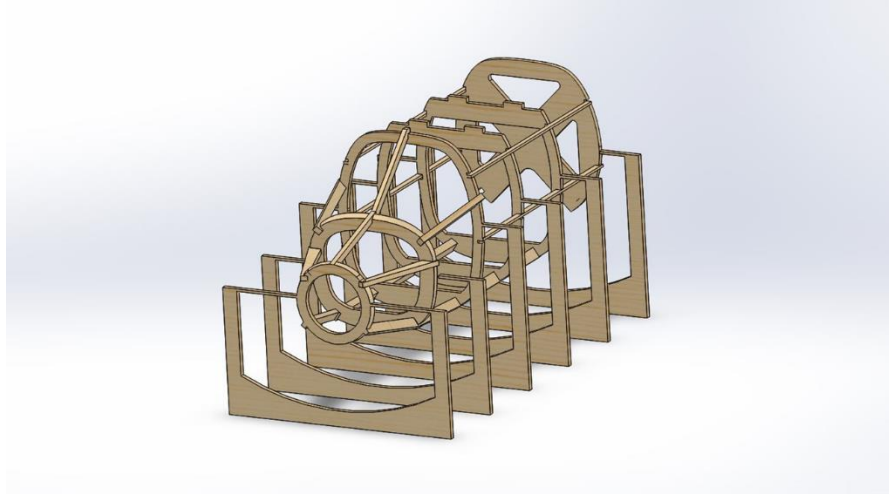


Figure 1: Dragonfly fuselage and jig frame CAD model

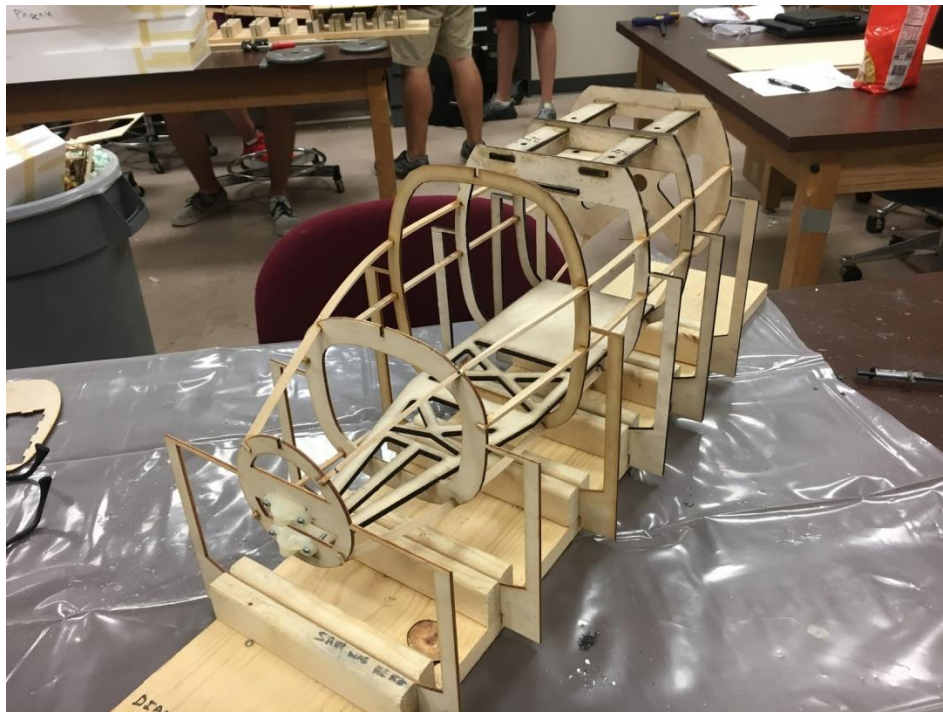


Figure 2: Dragonfly fuselage under construction



Figure 3: Dragonfly fuselage under construction

The exhaust port doubles as the wind tunnel sting's insert location. The sting's top surface lies flush with the bottom surface of the wing box. Six screws are inserted from the top of the wing, through the wing box and into the sting to anchor the aircraft to the wind tunnel setup. Figure 4 shows how the wind tunnel sting inserts into the fuselage. Figures 5 and 6 show the Dragonfly in the LSWT.

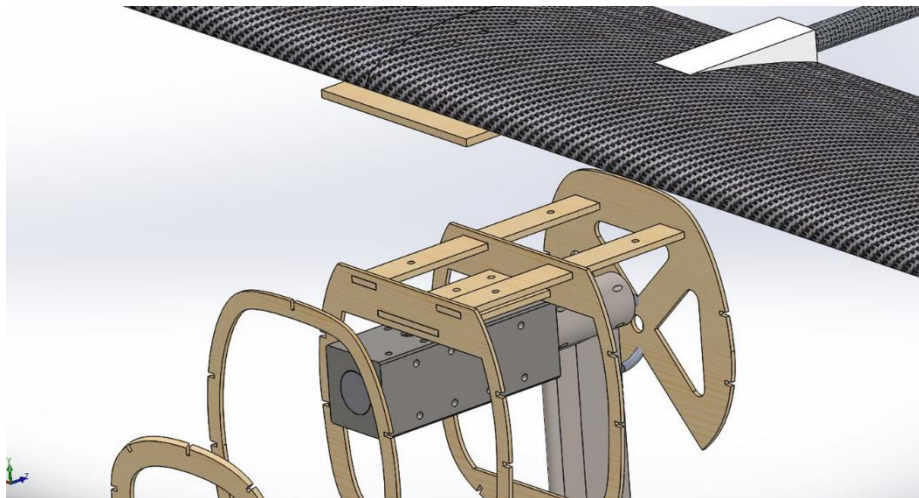


Figure 4: Wind tunnel sting inside the aircraft fuselage CAD view

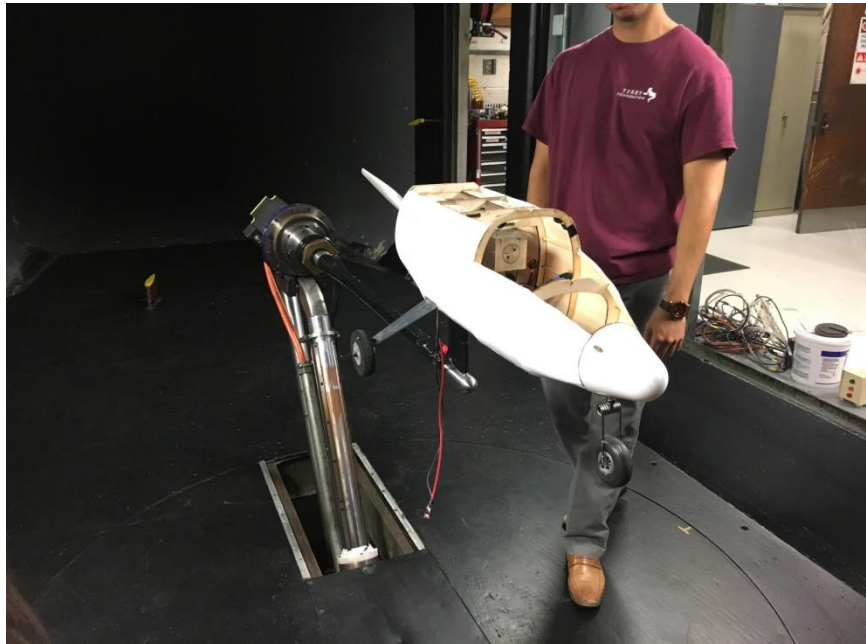


Figure 5: Wind tunnel sting inside the aircraft fuselage



Figure 6: Full aircraft setup in LSWT

Wind Tunnel Tests:

The Dragonfly's wind tunnel tests were conducted at the Oran W. Nicks Low Speed Wind Tunnel (LSWT) in College Station, Texas. The LSWT features a 7 foot by 10 foot test section, as well as a machine shop and various support rooms (Figure 7).

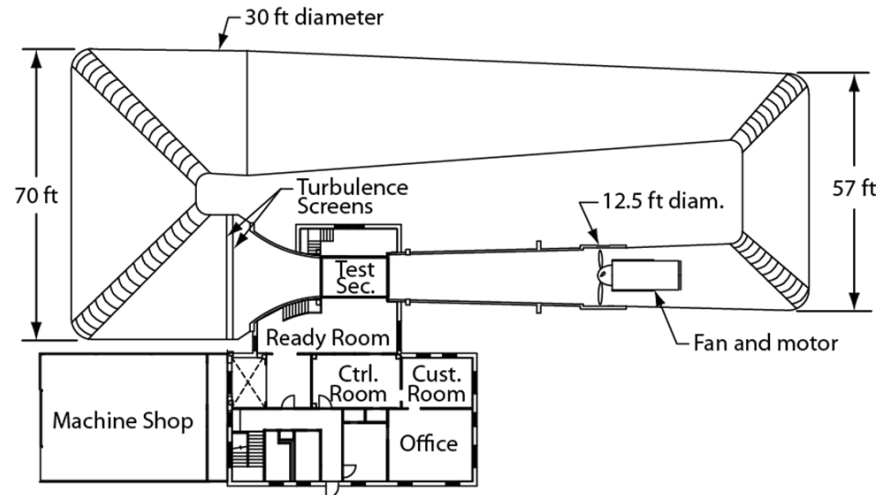


Figure 7: LSWT layout

The Dragonfly was secured to a high-alpha robot sting (HARS) motor capable of roll, pitch and yaw maneuvers. The sting is mated to an internal balance which measures forces and moments over six degrees of freedom (DOF) in the body frame. ATLAS used a Task Mark XIII balance. Table 4 lists the Mark XIII's measurement specifications.

Table 5: Task Mark XIII measurement ranges and uncertainties (body frame)

Measurement	Range and uncertainty
Diameter	1.25 in
N1, N2	500 lb \pm 0.4 lb
S1, S2	500 lb \pm 0.5 lb
Axial force	150 lb \pm 0.1 lb
Rolling moment	800 in-lb \pm 1.7 in-lb
Pitching moment	2625 in-lb
Yawing moment	2125 in-lb

Test Matrix and Test Procedures:

A series of aircraft orientation and wind velocity sweeps were performed to accomplish the wind tunnel test objectives listed in Table 1. A list of symbols and values relevant to the wind tunnel test matrix are shown in Table 5.

Table 6: Wind Tunnel test symbols and values

Parameter	Symbol	Range or Value
Takeoff dynamic pressure	Q1	qbar at 30 mph
Cruise dynamic pressure	Q2	qbar at 50 mph
Dynamic pressure range	QSweep	25:5:60 mph
Cruise alpha	Acruise	0 degrees
Pitch angle range	A1	-5:2:14 degrees
Yaw angle range	Y1	-4:1:10 degrees
Aileron deflection range	Aileron Sweep	Left to right; full, half, 0, half, full
Elevator deflection range	Elevator Sweep	Down to up; full, half, 0, half, full
Rudder deflection range	Rudder Sweep	Left to right; full, half, 0, half, full
Elevator max deflection	MaxElevator	30 degrees
Rudder max deflection	MaxRudder	30 degrees
Engine max throttle	Emax	100% throttle
Engine cruise throttle	Ecruise	--
Engine throttle sweep	Esweep	[0, 50, 100] % throttle

Aerodynamic and longitudinal behavior testing

A static tare measured the aircraft's CG and weight contribution to the measured normal and axial forces. The Dragonfly underwent alpha sweeps at takeoff and cruise conditions to understand the vehicle's performance. A dynamic pressure sweep at cruise alpha proved the Dragonfly's Reynold's number independence. Once Reynold's independence was established, all further wind tunnel tests were conducted at cruise dynamic pressure.

Run	Q	Pitch	Yaw	Controls	Comments
1	0	A1	0	NA	Wind-off static tare
2	QSweep	Acruise	0	NA	Reynold's independence check
3	Q2	A1	0	NA	Alpha sweep at cruise

Directional stability testing

Directional stability was measured with yaw sweeps at takeoff and cruise conditions to measure yaw-moments due to sideslip. This data was used to calculate the weathercock stability coefficient and the lateral stability coefficient.

Run	Q	Pitch	Yaw	Controls	Comments
4	Q2	Acruise	Y1	NA	Yaw sweep at cruise

Control surface effectiveness

The Dragonfly's control surfaces were deflected at takeoff and cruise conditions to verify their sizing and how effective they are at changing roll, pitch and yaw moments. Control effectiveness coefficients for the ailerons, elevator and rudders ($C_{l\delta_{Aileron}}$, $C_{m\delta_{Elevator}}$, $C_{n\delta_{Rudder}}$) were calculated from the gathered data.

Run	Q	Pitch	Yaw	Controls	Comments
5	Q1	Atakeoff	0	Elevator sweep	Elevator sweep at takeoff
6	Q2	Acruise	0	Aileron Sweep	Aileron sweep at cruise
7	Q2	Acruise	0	Elevator Sweep	Elevator sweep at cruise
8	Q2	Acruise	0	Rudder Sweep	Rudder sweep at cruise

Engine and propeller effects on control surface effectiveness

Wind tunnel testing with the engine and propeller installed were conducted to evaluate the effects of propwash on vehicle aerodynamics. Control surface effectiveness was measured at cruise conditions to evaluate any propwash effects.

Propwash effects are a particular concern to ATLAS since the Dragonfly has a pusher-prop configuration. Engine throttle sweeps at elevator and rudder full deflections determined if propwash changes their effectiveness.

Run	Q	Pitch	Yaw	Controls	Engine	Comments
9	Q2	Acruise	0	MaxElevator	Esweep	Max elevator deflection at cruise with engine throttle sweep. First two points at full elevator up; last two at full elevator down.
10	Q2	Acruise	0	MaxRudder	Esweep	Max rudder deflection at cruise with engine throttle sweep. First two points at full rudder left. Last two at full rudder right.

Theoretical results:

Aerodynamic analysis of the scaled Dragonfly was conducted with XFLR, an analysis tool for airfoils, wings and planes operating at low Reynolds Numbers. The XFLR results shown below give a first look at what type of results ATLAS may expect from the Dragonfly's wind tunnel tests.

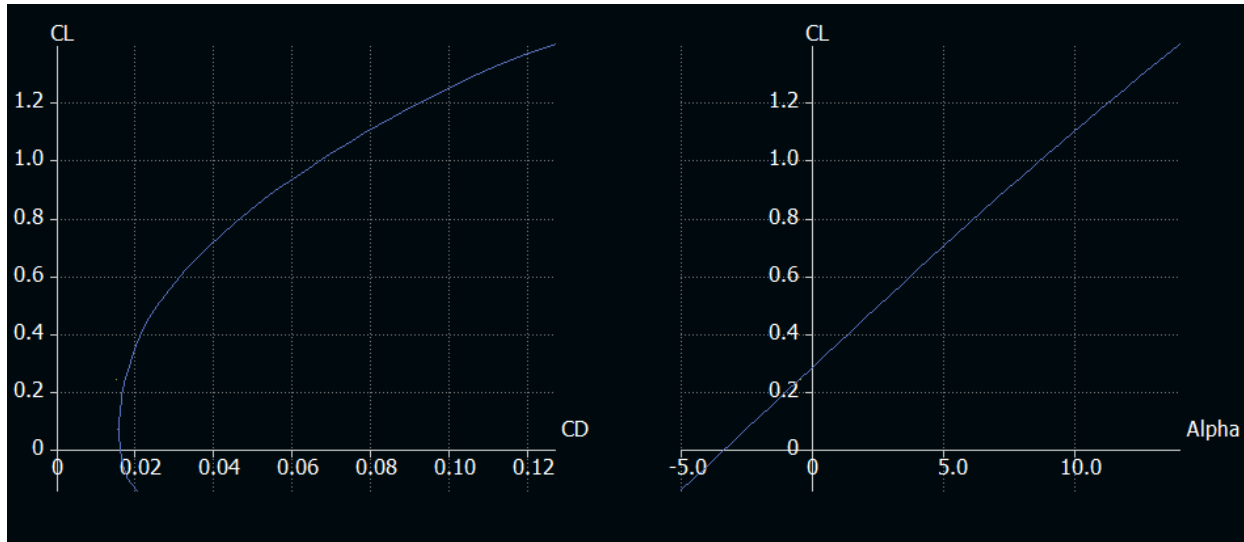


Figure 8: XFLR alpha sweep results – CL vs CD and CL vs Alpha sweep

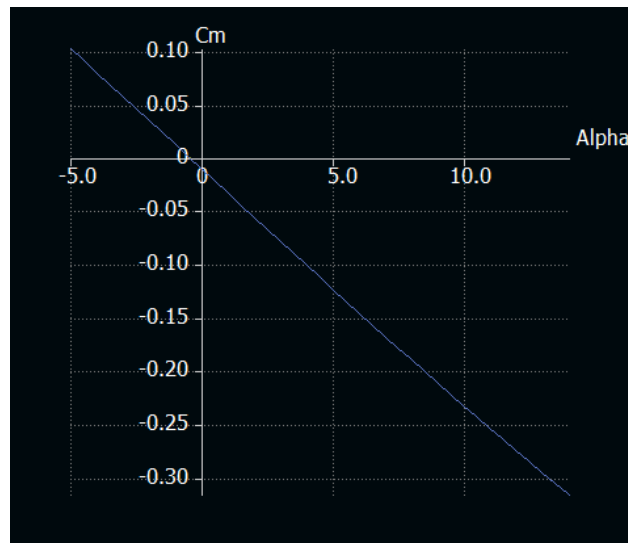


Figure 9: XFLR alpha sweep results – CM vs Alpha

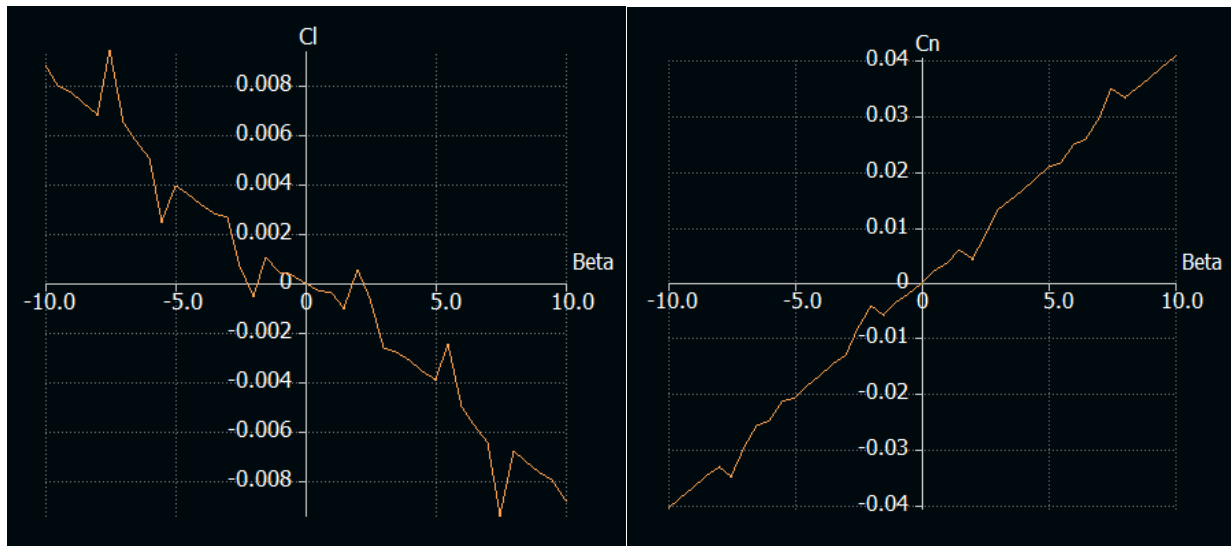


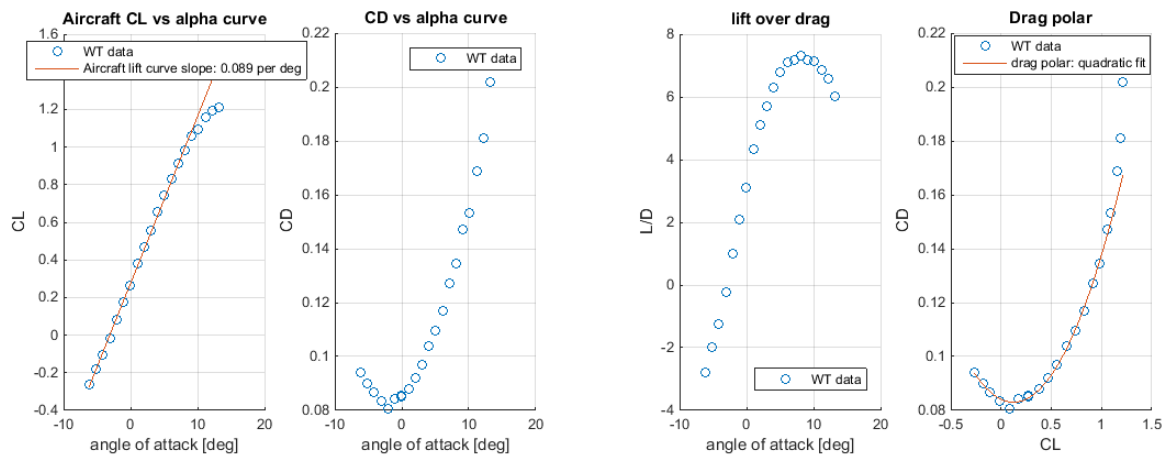
Figure 10: XFLR rolling, yawing moment coefficients versus beta angle sweep

Results and discussion:

The wind tunnel data was post-processed as described in the “data processing and background” section using a Matlab program suite developed by ATLAS. The program suite has been open-sourced and is available on Github (Appendix A). The results are presented below, followed by discussion on their values and calculations as applicable.

Lift and drag analysis:

Lift and drag characteristics for the Dragonfly were calculated with data gathered from run 3, an alpha sweep at cruise conditions. Figures 11 and 12 plot the collected data and fit trend lines when applicable.



Figures 11 and 12: Dragonfly lift and drag characteristics

Table 7 lists the wind tunnel data analysis results for the Dragonfly’s lift and drag performance.

Table 7: Lift and drag values

Characteristic	Value	Unit
$C_{L\alpha}$	0.089	Per deg
C_{Lmax}	1.212	-
$\alpha_{zerolift}$	-3.265	Deg
$\alpha_{critical}$	13.19	Deg
$C_{Dzerolift}$	0.084	-
C_{Dmin}	0.083	-
$C_{LminDrag}$	0.115	-
Oswalds efficiency factor e	0.615	-
LoD max	7.319	-
α_{LoDmax}	8.134	deg

A drag polar curve was approximated with the following analytical equation:

$$C_D = C_{D_{min}} + \frac{1}{\pi e AR} (C_L - C_{L_{minDrag}})^2$$

Every term except Oswald's efficiency factor can be determined from wind tunnel data. Oswald's efficiency factor was estimated using an area minimization technique. A quadratic curve was fit to the experimental drag polar and the area beneath this curve was calculated. Several values of e were plugged into the drag polar expression above, and the area beneath each curve was tabulated. The value of e that resulted in the smallest area difference between the fitted and analytical curves was taken to be the best value. Figure 13 illustrates this area minimization technique for three values of e .

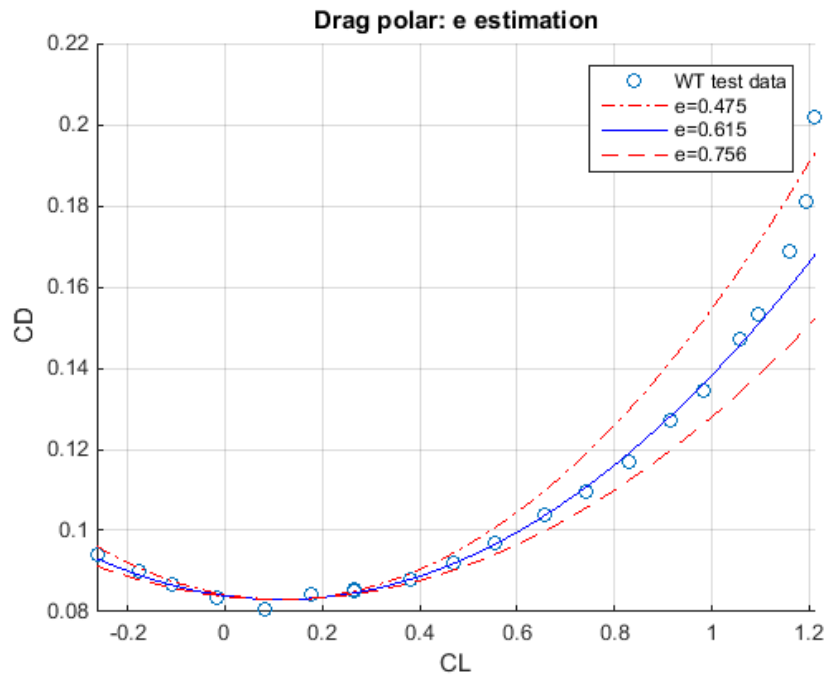


Figure 13: e calculation using area minimization

Note that the traditional equation:

$$C_D = C_{D_0} + \frac{C_L^2}{\pi e AR}$$

Does not work because it assumes the zero lift drag coefficient is equal to the minimum drag coefficient. This is not the case for the Dragonfly or for many aircraft.

Aircraft stability

Stability characteristics were calculated with data gathered from runs 3 and 4, alpha and beta sweeps at cruise conditions. Figure 14 plots aircraft moments versus alpha or beta with trend lines that calculate the three prime stability derivatives -- C_{m_α} , C_{n_β} , and C_{l_β} .

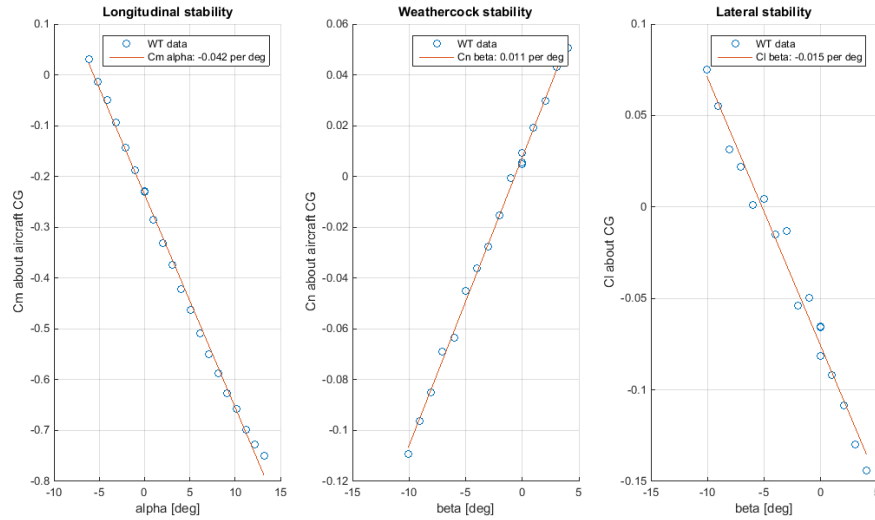


Figure 14: Dragonfly stability curves

The stability derivatives, the aerodynamic center and the static margin are listed in Table 8. Note that their values correspond to the stability sign criteria set forth in Table 2.

Table 8: stability values

Characteristic	Value	Unit
$C_{m\alpha}$	-0.042	Per deg
Weathercock stability $C_{n\beta}$	0.011	Per deg
Lateral stability $C_{l\beta}$	-0.015	Per deg
x_{ac}	1.683	Ft
SM	7.7	percent

Control surface effectiveness

Runs 6 through 8 were used to calculate control surface effectiveness. Note the following conventions for control surface deflections, listed in Table 9. Figure 15 plots control surface wind tunnel data.

Table 9: control surface deflection conventions:

Control surface	Convention
Elevator	(+) deflection → trailing edge down → More lift → Pitch down, counterclockwise moment → (-) C_m
Aileron	(+) deflection → roll right → Left aileron down, right aileron up
Rudder	(+) deflection → clockwise deflection → (+) side force → (-) moment about z

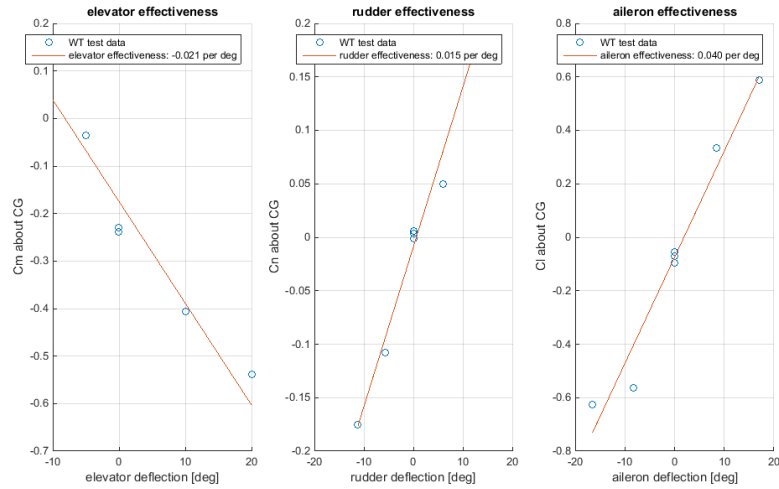


Figure 15: Control surface effectiveness

Table 10 lists the control surface effectiveness derivatives.

Table 10: control surface effectiveness:

Characteristic	value	Unit
Aileron effectiveness $C_{l_{\delta_{Aileron}}}$	0.04	Per deg
Elevator effectiveness $C_{m_{\delta_{Elevator}}}$	-0.021	Per deg
Rudder effectiveness $C_{n_{\delta_{Rudder}}}$	0.015	Per deg

Propwash effects

Runs 9 and 10 calculated propwash effects. The results are in Figure 16 and 17.

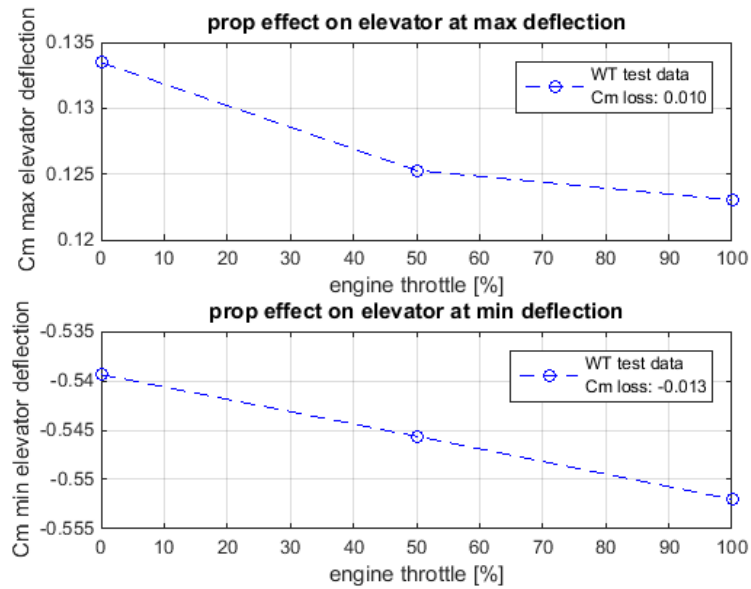


Figure 16: prop wash effects on elevator

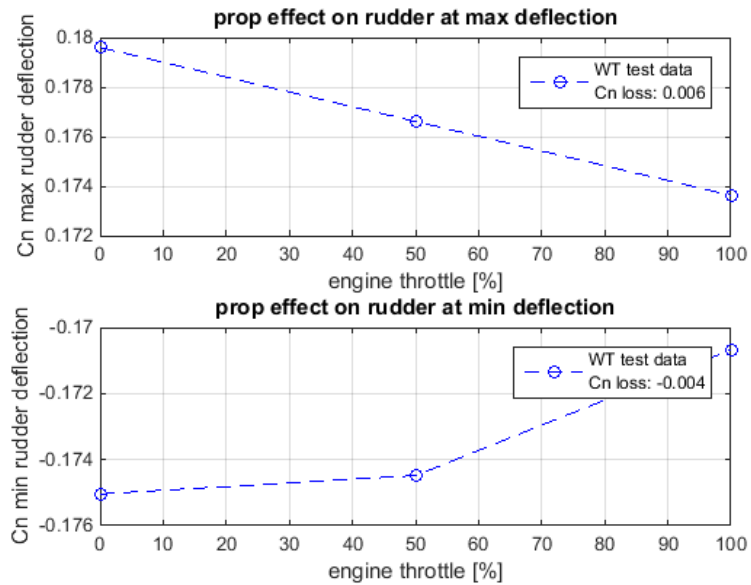


Figure 17: prop wash effects on rudders

As figures 16 and 17 show, prop wash does have an effect but the effect is negligible. Table 11 sums up the difference in moments the two control surfaces generate with zero engine throttle and max engine throttle.

Table 11: moment difference at zero and max throttle

Characteristic	Value
Elevator max deflection Cm loss	0.01
Elevator min deflection Cm loss	-0.013
Rudder max deflection Cn loss	0.006
Rudder min deflection Cn loss	-0.004

Appendix A: Wind tunnel analysis description and Github repository

The data read and post-processing code was developed to be easily expandable and applicable to a wide variety of aerodynamic analysis. It has been open-sourced at [github.com](https://github.com/rangelonline/RC-aircraft-wind-tunnel-analysis) for possible collaboration with other wind tunnel projects.

Github information:

User: `rangelonline`

Repository URL: [https://github.com/rangelonline/RC-aircraft-wind-tunnel-analysis.git](https://github.com/rangelonline/RC-aircraft-wind-tunnel-analysis)